Immunity 25, 285–295, August 2006 ©2006 Elsevier Inc. DOI 10.1016/j.immuni.2006.06.014

Impaired Integrin-Dependent Function in Wiskott-Aldrich Syndrome Protein-Deficient Murine and Human Neutrophils

Hong Zhang,[1] Ulrich Y. Schaff,[4] Chad E. Green,[4] Hua Chen,[2] Melissa R. Sarantos,[4] Yongmei Hu,[1] Diane Wara,[3] Scott I. Simon,[4] and Clifford A. Lowell[1,*]
[1] Department of Laboratory Medicine
[2] Department of Medicine
[3] Department of Pediatrics
University of California, San Francisco
San Francisco, California 94143
[4] Department of Biomedical Engineering
University of California, Davis
Davis, California 95616

Summary

Wiskott-Aldrich syndrome (WAS) is a primary immunodeficiency that manifests as increased susceptibility to many pathogens. Although the spectrum of infections suffered by WAS patients is consistent with defects in neutrophil (PMN) function, the consequences of WAS protein (WASp) deficiency on this innate immune cell have been unclear. We report that deficiency of WASp in both human and murine PMNs resulted in profound defects in clustering of β2 integrins, leading to defective adhesion and transendothelial migration under conditions of physiologic shear flow. Wild-type PMNs redistributed clustered β2 integrins to the uropod of the cell during active migration, whereas WASp-deficient cells remain unpolarized. The WASp-deficient PMNs also showed reduced integrin-dependent activation of degranulation and respiratory burst. PMNs from a WAS patient manifested similar defects in integrin clustering and signaling. These results suggest that impaired β2 integrin function in WASp-deficient PMNs may contribute substantially to the clinical immunodeficiency suffered by WAS patients.

Introduction

The Wiskott-Aldrich syndrome (WAS) is an X-linked primary immunodeficiency caused by genetic mutations within the Wiskott-Aldrich protein (WASp). WAS patients develop a variety of bacterial, viral, and fungal infections (Burns et al., 2004a). WASp, which is exclusively expressed in hematopoietic cells, is important in regulating actin cytoskeletal dynamics (Badour et al., 2004). Its role in regulating blood cell shape, polarity, and migration underlies many of the clinical manifestations of the disease. WASp-deficient mice are not as severely affected as WAS patients, but many of the cellular defects first observed in WAS patients have also been observed in $Was^{-/-}$ mice, thereby confirming that the knockout animals are a good model of the disease (Snapper et al., 1998; Zhang et al., 1999).

*Correspondence: clifford.lowell@ucsf.edu

Despite the fact that most WAS patients suffer from infections that are often associated with neutrophil (PMN) dysfunction, the role of WASp in PMN biology has been poorly studied. Early studies in WAS patients revealed partial impairments in PMN chemotaxis; however, they were correctable with normal serum, implying that the defect was not intrinsic to the PMN (see Burns et al., 2004a). With more modern approaches of observing directed chemotaxis in Dunn chambers, PMNs from WAS patients showed both normal directional and speed of migration responses to classical chemoattractants such as formyl peptides and interleukin-8 (Zicha et al., 1998). No obvious defects have been reported in PMN adhesive function in either WAS patients or $Was^{-/-}$ mice. However, impaired phagocytosis of yeast zymosan particles has been observed in $Was^{-/-}$ murine PMNs (Zhang et al., 1999).

In contrast, the contribution of PMN dysfunction to the immunodeficiencies caused by leukocyte adhesion deficiency (LAD) syndromes LAD I, LAD II, and LAD III is well understood (Bunting et al., 2002). Each of these diseases is characterized by impaired adhesion, migration, and accumulation of PMNs at sites of infection, leading to chronic infections. The pathophysiology of LAD I and LAD III are directly attributable to β2 integrin dysfunction in PMNs, either due to loss of integrin expression (LAD I) or reduction in the ability to activate integrin affinity and avidity changes via deficiency of Rapl GTPase (LAD III). It is reasonable to assume that impairment of PMN integrin function via loss of other signaling molecules, such as WASp, could be a major contributor to immunodeficiency.

Defects in mononuclear cell adhesion and migration have been reported in both WAS patients and $Was^{-/-}$ mice. Mononuclear cells from WAS patients display profound defects chemotactic responses, potentially resulting from disruption of podosome formation (Badolato et al., 1998). Correlated with a lack of podosomes, WASp-deficient human dendritic cells (DCs) fail to cluster their β2 integrins, and as a result these cells have reduced adhesion to intracellular adhesion molecule 1 (ICAM-1) under conditions of fluid shear stress (Burns et al., 2004b). In $Was^{-/-}$ mice, the inability of DCs to form proper adhesion contacts leads to impaired migratory responses from sites of antigen deposition to regional lymph nodes (de Noronha et al., 2005).

We have examined the role of WASp in PMN function by using both $Was^{-/-}$ mice and cells from a WAS patient. WASp-deficient murine PMNs displayed a substantial defect in integrin clustering and redistribution to the contact area during attachment to ligand-coated surfaces (or endothelial monolayers), leading to impaired adhesion and reduced integrin-dependent activation. Similar results were observed examining human PMNs from a WAS patient. The reduced capacity of WASp-deficient PMNs to form high-avidity β2 integrin adhesive contacts may be a major contributor to the immunodeficiency present in WAS patients.

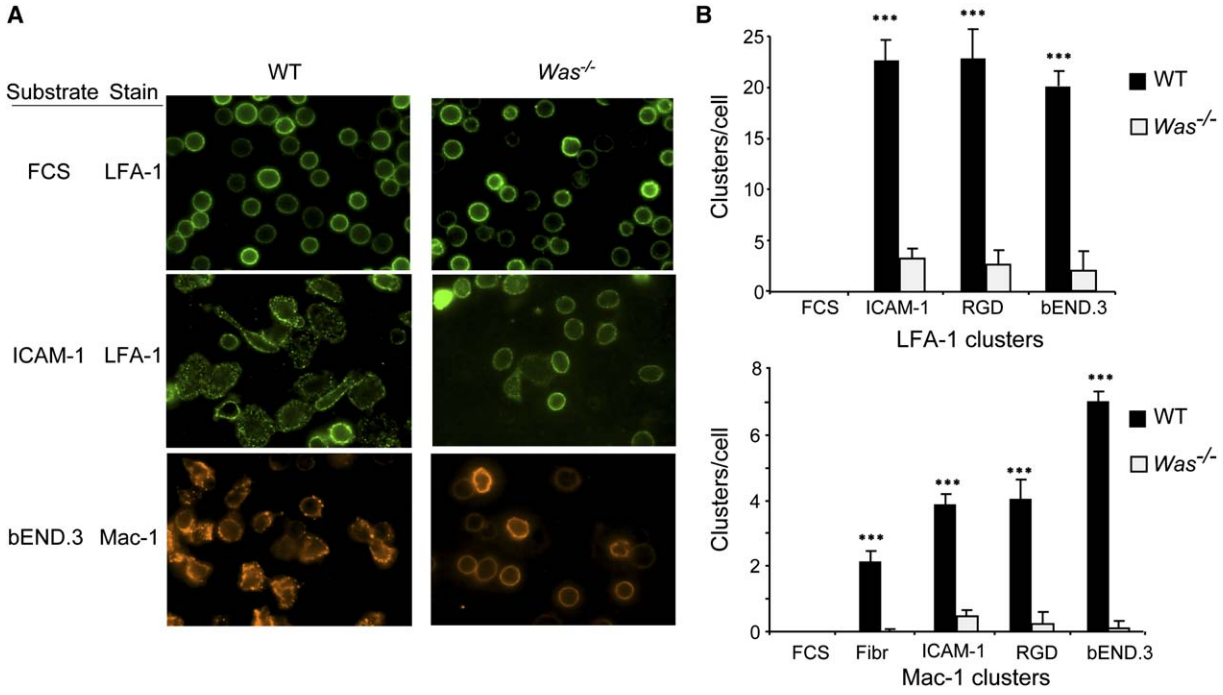

Figure 1. WASP-Deficient PMNs Fail to Cluster LFA-1 and Mac-1 during Adhesion under Static Conditions

(A) Wild-type and *Was*$^{-/-}$ PMNs were plated on glass coverslips coated with FCS or ICAM (10 min) or on monolayers of cultured TNF-α-activated bEND.3 cells (20 min), in the absence of fluid shear stress, and then fixed and stained with anti-CD11a (LFA-1) or biotinoylated anti-CD11b (Mac-1) followed by Alexa448-conjugated secondary Ab or Alexa594-conjugated streptavidin.

(B) Quantification of integrin clustering for either LFA-1 (left) or Mac-1 (right) in wt versus *Was*$^{-/-}$ cells. Cells were plated on the indicated surfaces, fixed and stained as shown in (A), and then clustered integrins were counted with Image J (NIH) analysis software. RGD, poly-RGD peptide coated; Fibr, fibrinogen coated. Data shown are averaged from three separate experiments counting 100 cells per experiment. Error bars are ± SD. ***$p < 0.001$ between wt and *Was*$^{-/-}$.

Results

Clustering of LFA-1 and Mac-1 Is Impaired in *Was*$^{-/-}$ PMNs

In WASp-deficient dendritic cells, reduced clustering of β2 integrins and poor podosome formation contributes to the diminished adhesive and migratory capacity of these cells (Burns et al., 2004b). Although neutrophils (PMNs) do not form podosome-like structures, they do cluster integrins during cell attachment. To address whether WASp is involved in this process, we examined integrin-clustering events in PMNs during static, i.e., nonshear flow, adhesion to extracellular matrix (ECM)-coated surfaces in wild-type (wt) versus *Was*$^{-/-}$ cells. Clustering of CD11a (LFA-1) or CD11b (Mac-1) was determined by immunofluorescence microscopy followed by image analysis. Resting PMNs plated on ligand-free surfaces displayed an even distribution of surface LFA-1 or Mac-1 (Figure 1A), confirming flow cytometry data (not shown) that showed equal expression of these integrins by *Was*$^{-/-}$ and wt cells. PMNs plated on various ligand-coated surfaces (fibrinogen, ICAM-1, poly-Arg-Gly-Asp [poly-RGD] peptide) or on tumor necrosis factor (TNF-α)-activated murine brain endothelial (bEND.3) cells under static conditions showed obvious integrin clustering that accompanied cell spreading (Figure 1A, with LFA-1 or Mac-1 cluster quantification shown in Figure 1B). Although *Was*$^{-/-}$ PMNs attached to the various ligand-coated surfaces, the cells remained predominately round and showed an 85%–95% reduction in integrin clustering (Figures 1A and 1B). These data indicate that WASp-deficient PMNs fail to reorganize their surface integrin molecules during attachment to adhesive surfaces under standard static, nonshear flow, conditions.

To obtain a more physiologically relevant view of integrin clustering during adhesion, we examined PMNs under flow conditions by using alternating differential interference contrast (DIC)—fluorescence video microscopy. Cells were stained with Alexa488-conjugated Mac-1 or non-blocking LFA-1 mAbs, then perfused over ICAM-1-coated coverslips a shear force of 0.3 dyne/cm^2. Under these conditions, the PMNs would attach and then spread over the adhesive surface and spontaneously begin to migrate (Figure 2 and Movies S1–S8 in the Supplemental Data available with this article online). In wt cells, the transition from attachment to fully spread and migrating cells occurred rapidly (usually less than 20 s). During this process, both LFA-1 and Mac-1 concentrated in the mid-hind region (uropod) of the migrating wt cell, whereas the leading edge (lamellopodia) was cleared of both integrins (Movies S2 and S4). Numerous punctuate regions of clustered integrins can be seen in the wt cells moving from the dense regions in the uropod toward the midregion of the cell during directional migration. In contrast, *Was*$^{-/-}$ PMNs failed to redistribute their LFA-1 or Mac-1 integrins to either side of the cell during attachment to ICAM-1 (Figure 2, Movies S6 and S8). Instead, in most of the *Was*$^{-/-}$ cells, both LFA-1 and Mac-1 tended to aggregate in the central

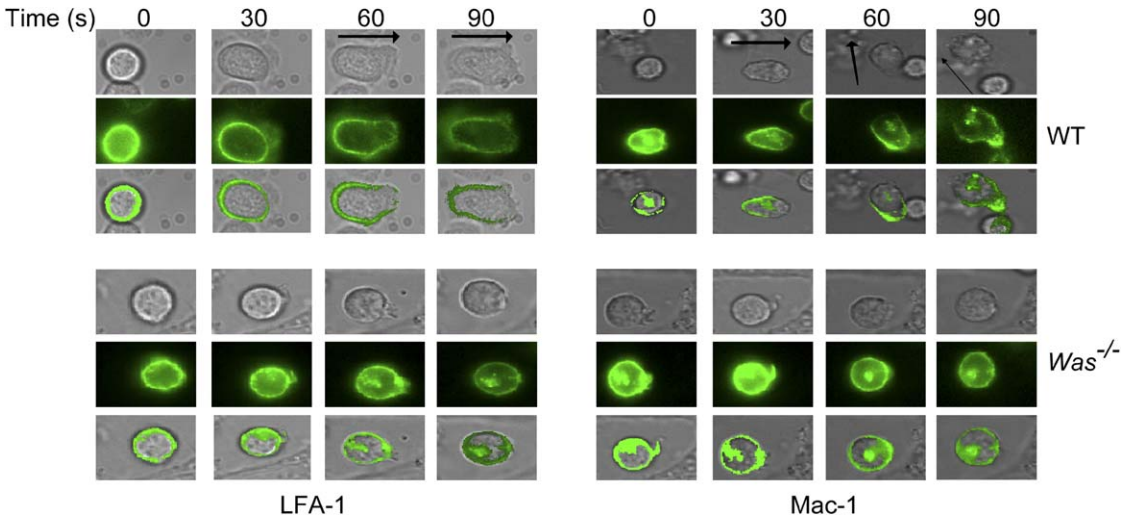

Figure 2. WASp-Deficient PMNs Have Impaired β2 Integrin Clustering during Adhesion under Shear Stress

Wild-type or *Was*$^{-/-}$ PMNs were stained with anti-Mac-1-Alexa488 or nonblocking anti-LFA-1-Alexa488, and then passed over coverslips coated with ICAM-1 at a shear stress of 0.3 dyne/cm^2 at room temperature. Continuous video imaging was acquired with 2 s alteration between DIC and fluorescence microscopy. Representative single-cell images were culled from various videos (at the indicated time frames) and overlaid. The top eight rows of images show wt cells, stained with anti-LFA-1 (left four) or anti-Mac-1 (right four) adhering and migrating (direction indicated by solid arrow). Lower panels show *Was*$^{-/-}$ cells.

region of the cell. Similar results were observed during attachment to other adhesive surfaces (fibrinogen, poly-RGD peptides, or bEND.3 cells; data not shown). Thus, under both static adhesion conditions and in response to physiologic shear force during perfusion over adhesive surfaces, WASp-deficient PMNs failed to reorganize their β2 integrins into clustered structures analogous to those seen in wt cells.

Was$^{-/-}$ PMNs Have Reduced Adhesion under Shear Stress

A potential consequence of impaired integrin clustering is reduced adhesive capacity of leukocytes. With standard binding assays done under static conditions, we failed to see substantial differences in the ability of *Was*$^{-/-}$ PMNs to adhere to ICAM- or poly-RGD-coated surfaces while delayed attachment was observed on fibrinogen (Figures S1A and S1B). As a more physiologic assessment of PMN adhesion, we examined the ability of wt versus WASp-deficient PMNs to roll, attach, and firmly adhere to monolayers of murine L-cells stably expressing E-selectin and ICAM-1 (L-EI cells) at a venular shear stress of 1 dyne/cm^2. Under these conditions, adhesion strengthening by integrin activation and membrane clustering is critical for stable PMN-L-EI cell interactions (Simon and Green, 2005). Under shear flow conditions, the number of PMNs interacting (either rolling or attached) with the L-EI monolayers was equivalent between wt and *Was*$^{-/-}$ cells (Figure 3A). Capture and rolling of PMNs was mediated by E-selectin because interactions were blocked by addition of E-selectin mAb but were unaffected by anti-ICAM-1 or LFA-1. Similarly, *Was*$^{-/-}$ PMNs captured and rolled normally on peripheral node addressin (PNAd)-coated surfaces, indicating that deficiency of WASp did not affect L-selectin-mediated cell attachment. However, the number of interacting *Was*$^{-/-}$ PMNs that transitioned to firmly arrested cells was reduced by 65% compared to wt PMNs, similar to effect seen with anti-ICAM or anti-LFA-1 treatment of wt cells. PMN firm adhesion to L-EI cells in this assay is dependent primarily on LFA-1, as Mac-1-deficient cells adhered normally. Together these data demonstrate that WASp-deficient PMNs are able to attach and roll normally over an E-selectin-expressing cell monolayer or over a PNAd-coated surface but that LFA-1-ICAM-1-mediated PMN firm arrest was substantially impaired.

In vivo chemokines and chemoattractants presented on the apical surfaces of endothelial cells can promote both adhesion and migration, depending on the density of integrin ligands on the endothethium (Cinamon et al., 2004). To determine whether the presence of an apically presented chemoattractant, such as platelet-activating factor (PAF), would mitigate the adhesive defect of *Was*$^{-/-}$ cells, we perfused PMNs over cellular monolayers pretreated with PAF. Addition of PAF did not affect the ability of L-EI cells to support PMN adhesion at 1 dyne/cm^2, whereas it did facilitate improved wt leukocyte adhesion to bEND.3 monolayers (Figure 3B). The capacity of *Was*$^{-/-}$ PMNs to adhere under shear flow was not improved by addition of PAF.

We next examined the capacity of WASp-deficient PMNs to form high-avidity adhesion clusters that could resist progressively increasing amounts of shear stress. For this experiment, PMNs were allowed to interact with TNF-α-activated bEND.3 cells at low shear (0.3 dyne/cm^2), and then the percentage of cells that remained firmly adherent at 1, 4, and 10 dyne/cm^2 was determined. The percentage of wt cells that were able to remain adherent at 4 and 10 dyne/cm^2 steps progressively increased over the number at the 1 dyne/cm^2 step, whereas the few *Was*$^{-/-}$ cells that arrested at 1 dyne/cm^2 were progressively washed away at the high shear (Figure 3C). The increase in % adherent cells in the wt

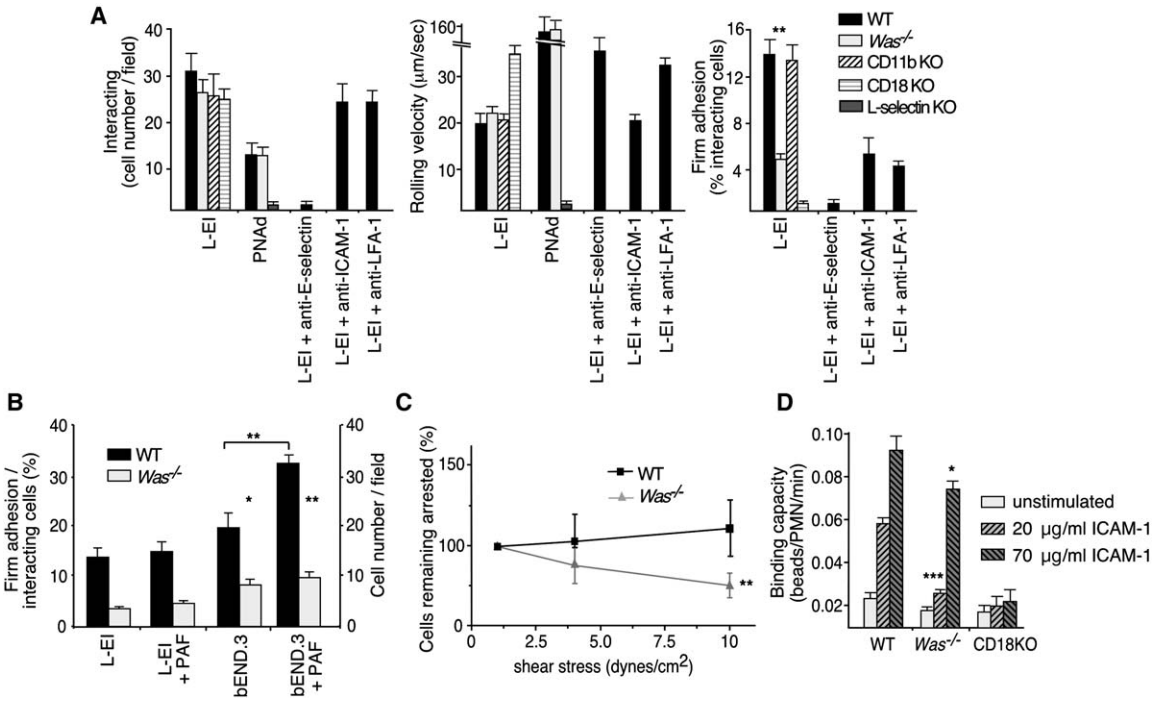

Figure 3. Impaired Adhesion of *Was*$^{-/-}$ PMNs under Shear Stress

(A) Wild-type, *Was*$^{-/-}$, CD11b (Mac-1)-deficient, CD18-deficient, or L-selectin-deficient PMNs were injected into a parallel plate flow chamber and passed over a monolayer of L-EI cells or PNAd-coated surfaces at a shear of 1 dyne/cm^2 for 1 min. Video recordings were then taken at 30 s intervals and the numbers of rolling or adherent cells were counted with Image Pro Plus v4.5 software. Interacting, rolling, or firmly adherent cells are defined in Experimental Procedures. In some experiments, PMNs were pretreated with anti-E-selectin, anti-ICAM-1, or blocking anti-CD11a (LFA-1) (10 μg/ml for 10 min) prior to injection into the flow cell.

(B) Wild-type and *Was*$^{-/-}$ PMNs were passed over monolayers of L-EI- or TNF-α-activated murine bEND.3 cells, either with or without preincubation with PAF (1 μM) for 5 min, at a shear of 1 dyne/cm^2 for 1 min, and the number of firmly adherent cells was counted. For both (A) and (B), data shown are mean ± SD, n = 3–5 separate microscopy fields and are representative of at least three independent experiments.

(C) Wild-type or *Was*$^{-/-}$ PMNs were allowed to interact with TNF-α-stimulated bEND.3 cell monolayer for 3 min at a shear force of 0.3 dyne/cm^2, after which the shear stress was ramped up to 1, 4, and 10 dyne/cm^2 for 1 min each. The total number of arrested cells in a given microscopy field were counted at each shear step, and the initial counts at the 1 dyne/cm^2 level were indexed as 100%. Data shown are mean ± SD, n = 3–5 separate microscopy fields.

(D) Wild-type, *Was*$^{-/-}$, or CD18-deficient PMNswere mixed with fluorescent microbeads that had been precoated with ICAM-1-Fc at either low density (20 μg/ml) or high density (70 μg/ml), then subjected to stirring at a rotary shear stress of 1 dyne/cm^2. The rate of bead capture onto the PMNs was determined by continuous flow cytometry from the stirring cells. After determination of bead binding in resting cells, the PMNs were stimulated by addition of 3 μM fMLP to activate high-affinity integrin binding. Data shown are mean ± SD, n = 3 and are representative of three independent experiments. KO, knockout, e.g., CD11b KO is CD11b-deficient. *p < 0.05, **p < 0.01, ***p < 0.001 compared to wt.

is due to rolling PMNs that entered the field of view during the 1 or 4 dyne/cm^2 step and then transitioned to fully adherent cells capable of resisting higher shear. Recruitment of *Was*$^{-/-}$ cells at higher shear was nearly absent. This indicates that the ability of *Was*$^{-/-}$ PMNs to strengthen adhesion contacts through LFA-1 clustering and formation of high-avidity interactions is considerably reduced compared to wt cells.

To further assess the ability of *Was*$^{-/-}$ PMNs to form stable adhesion contacts, we used a flow cytometric-based bead binding assay performed under rotational shear of 1 dyne/cm^2 (Lum et al., 2002). The rate of ICAM-1 bead capture by *Was*$^{-/-}$ PMNs was significantly reduced compared to wt cells, especially with beads coated at a lower density of ICAM-1 (Figure 3D). Both types of PMNs showed a dramatically increased rate of bead binding after stimulation by fMLP, whereas control CD18-deficient PMNs failed to bind beads at all. These data confirm that, especially at low ICAM-1 site density, *Was*$^{-/-}$ PMNs manifest decreased LFA-1-mediated adhesion capacity under shear stress.

Was$^{-/-}$ PMNs Have Reduced Migratory Capacity In Vitro and In Vivo

An obvious implication of the reduced adhesive capacity of WASp-deficient PMNs should be reduced integrin-dependent migratory ability. However, previous studies had indicated that PMNs from WAS patients display normal speed and direction of motility in gradients of fMLP or IL-8 within Dunn chemotaxis chambers (Zicha et al., 1998). Indeed, in standard Transwell chamber type chemotaxis assays, we found that murine *Was*$^{-/-}$ PMNs also migrated normally in response to MIP-1α, MIP-2, or fMLP (Figure S1C). Under similar static conditions, *Was*$^{-/-}$ PMNs displayed no defect in their ability to transmigrate through monolayers of murine bEND.3 cells in response to chemokine stimulation (Figure S1D). However, given that the major defect in integrin-dependent adhesion in *Was*$^{-/-}$ PMNs was apparent only under shear stress, we examined the ability of WASp-deficient cells to transmigrate through a monolayer of bEND.3 cells in parallel plate flow assays. Approximately 30% of the adherent wt cells accomplished

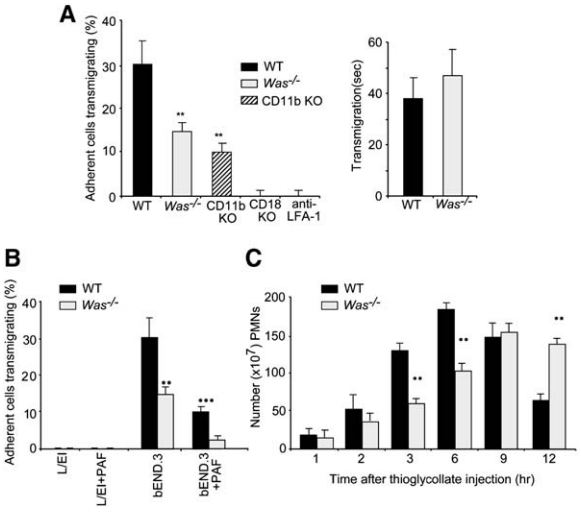

Figure 4. *Was*$^{-/-}$ PMNs Display Reduced Transendothelial Migration In Vitro and In Vivo

(A) Wild-type, *Was*$^{-/-}$, CD11b (Mac-1)-deficient or CD18-deficient PMNs were injected into a parallel plate flow cell and passed over a monolayer of TNF-α-activated murine bEND.3 cells at a shear of 0.3 dyne/cm^2 for 1 min to promote adhesion, then ramped up to 1 dyne/cm^2, after which cells observed for rolling, adhesion, and transmigration. Transmigration was quantitated by counting the phase dark PMNs that migrated beneath the endothelium and out of the focal plane. The numbers of adherent cells that transmigrated through the endothelial cell monolayer were counted over a total of 15 microscopy fields (total transmigrated cells counted ~50–60 in wt) and divided by the number of adherent cells in each field to obtain the percentage transmigrating. In some experiments, anti-CD11a was injected with the PMNs. Right panel shows the average time for transmigration.

(B) Wild-type and *Was*$^{-/-}$ PMNs were passed over monolayers of L-EI- or TNF-α-activated murine bEND.3 cells, either with or without preincubation with PAF (1 μM) for 5 min, at a shear of 0.3 dyne/cm^2 for 1 min, and the percentage of firmly adherent cells that transmigrated through the monolayers was counted. For both (A) and (B), data shown are mean ± SD, n = 3 PMN injections and representative of at least two independent experiments.

(C) Wild-type or *Was*$^{-/-}$ littermates mice were injected i.p. with 3% thioglycollate, and the number of PMNs in peritoneal lavage fluid at 1, 2, 3, 6, 9, and 12 hr later was determined by flow cytometry (double staining for CD45.2/Gr1). Data shown are based on 5 mice per group and is representative of three independent experiments. Error bars are ± SD. **p < 0.01, ***p < 0.001 compared to wt.

complete transmigration, while only 15% of the adherent *Was*$^{-/-}$ or Mac-1-deficient cells transmigrated, though duration from arrest to crossing the endothelium was equivalent in both cell types (Figure 4A). Transmigration was completely absent in CD18-deficient PMNs or after blockade of wt cells with anti-LFA-1, as these cells failed to adhere at all to the bEND.3 monolayer. Pretreatment of the bEND.3 cells with PAF lowered migration of both wt and *Was*$^{-/-}$ cells, potentially due to increased adhesion, but failed to rescue the relative deficiency in the *Was*$^{-/-}$ cells (Figure 4B). These observations demonstrate that under physiologic levels of shear stress, *Was*$^{-/-}$ PMNs manifest reduced adhesive and migratory capacity.

To examine the ability of *Was*$^{-/-}$ cells to migrate in vivo, we used the thioglycollate peritonitis model. At various time points after peritoneal installation of 3% sterile thioglycollate, invading PMNs were enumerated by Gr-1 and CD45 staining followed by flow cytometry. WASp-deficient mice showed a clear delay in migration of PMNs into the inflamed peritoneum compared to wt littermate control animals (Figure 4C). At later time points, as more macrophages enter the inflammatory site, PMN numbers dropped in wt animals but remained high in *Was*$^{-/-}$ mice, consistent with the known defect in macrophage migration caused by WASp deficiency (Jones et al., 2002).

Was$^{-/-}$ PMNs Have Reduced Integrin-Dependent Functional Responses

Of the two main β2 leukocyte integrins, LFA-1 plays a greater role in leukocyte rolling, adhesion, and migration, whereas Mac-1 is more involved in leukocyte activation after adhesion (Ding et al., 1999). Because the integrin-clustering defect in *Was*$^{-/-}$ PMNs affected Mac-1 as much as LFA-1, we chose to examine leukocyte activation by adhesion as a better gauge of the functional defects that may result from impaired Mac-1 (or β1/β3 integrin) signaling. Adhesion-mediated degranulation of *Was*$^{-/-}$ PMNs was reduced to near background (similar to Mac-1-deficient cells) after plating on either collagen- or fibrinogen-coated surfaces (Figure 5A). In contrast, when these cells were stimulated with PMA, which directly activates functional responses in the absence of adhesion, all cell types responded equivalently, indicating that the *Was* mutation does not affect the general machinery of degranulation.

Similar to degranulation, *Was*$^{-/-}$ cells showed significantly reduced activation of respiratory burst after plating on serum-, fibrinogen-, poly-RGD-, or ICAM-1-coated plates (Figure 5B). We were also able to detect a much weaker respiratory burst when PMNs were plated directly on TNF-α-stimulated bEND.3 cells; in this assay, the *Was*$^{-/-}$ cells were completely defective. As a control, we also examined the degranulation and respiratory burst responses of *Was*$^{-/-}$ PMNs in suspension (nonadhesive conditions) after activation with a number of G protein-coupled receptor (GPCR) agonists (fMLP, PAF, LTB4, and C5a). In all cases, adhesion-independent activation of *Was*$^{-/-}$ PMNs was normal (Figure S2), demonstrating that the mutation does not intrinsically affect the function of the NADPH oxidase or the major intracellular signaling pathways from these GPCRs. However, as expected, GPCR-induced activation of actin polymerization in suspended PMNs was significantly reduced in the *Was*$^{-/-}$ cells (Figure S3).

Reduced Adhesion and Activation of PMNs from a Wiskott-Aldrich Syndrome Patient

To validate that the *Was*$^{-/-}$ mice represent a good model for PMN defects that may be present in human WAS patients, we analyzed integrin clustering, adhesion under shear flow, and integrin-mediated activation of cells from a WAS donor. The patient has a point mutation in the *WAS* gene (R86C), a common hotspot for substitution mutations that are often associated with more severe immunodeficiency (Kolluri et al., 1995). In this patient, the amount of WASp in PMNs was less than 10% of normal (Figure 6A). Peripheral blood PMNs from this patient showed a marked impairment in integrin clustering when plated on human ICAM-1-coated surfaces, resembling the phenotype seen in murine *Was*$^{-/-}$ cells

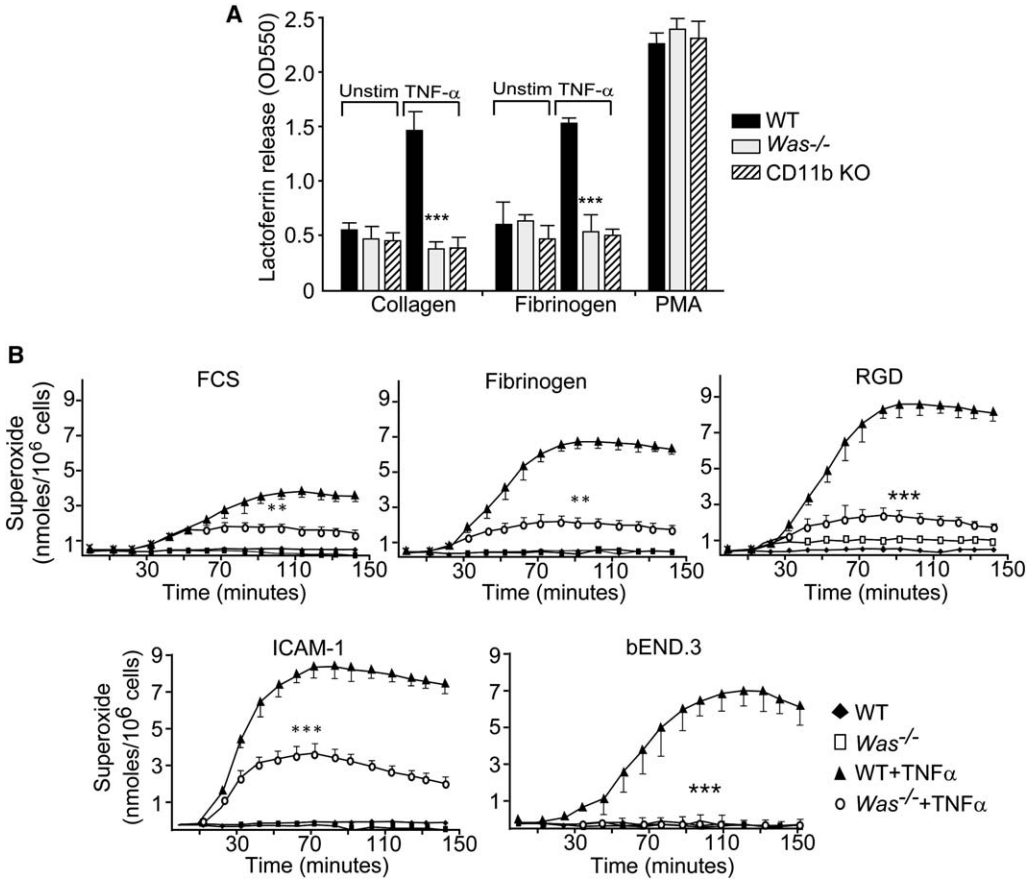

Figure 5. *Was*$^{-/-}$ PMNs Display Impaired Integrin-Mediated Degranulation and Respiratory Burst Responses

(A) Wild-type, *Was*$^{-/-}$, and CD11b (Mac-1)-deficient PMNs were plated in microtiter wells precoated with either collagen or fibrinogen, in the presence or absence of TNF-α (10 ng/ml), then cultured for 90 min. Release of the secondary granule marker lactoferrin into the cell supernatant was determined by ELISA. Data are mean ± SD, n = 6 wells each and are representative of three independent experiments. In some samples, PMA (1 nM) was added as a pharmacologic activator of PMN degranulation.

(B) Wild-type and *Was*$^{-/-}$ PMNs were plated on microtiter wells coated with the indicated ligands (RGD, polyRGD peptide) or containing a monolayer of TNF-α-treated bEND.3 cells, in cytochrome C media with and without TNF-α (10 ng/ml). Production of superoxides by respiratory burst was measured as reduction of the cytochrome C. Data are mean, n = 3 wells each and are representative of at least three independent experiments. Error bars are ± SD. **p < 0.01, ***p < 0.001 compared to wt.

(Figure 6B). In parallel plate shear flow assays, the PMNs from this patient rolled normally on both TNF-α-stimulated HUVEC and L-EI cells but demonstrated a clear defect in arrest and firm adhesion (Figure 6C). The PMNs from this patient also had an obvious defect in adhesion-dependent activation of respiratory burst after plating on human ICAM-1-, fibrinogen-, or poly-RGD peptide-coated surfaces (Figure 6D). These data demonstrate that in at least one individual, WASp deficiency affects integrin function similarly in human and murine PMNs.

Reduced Integrin-Dependent Signaling Events in *Was*$^{-/-}$ PMNs

Clustering of integrins after ligand binding initiates both a Ca^{2+} flux and downstream phosphorylation of many proteins, including tyrosine kinases such as Syk and Pyk2, their substrates such as Vav and Cbl (which lead to activation of the Erk1 and Erk2 pathway), and anti-apoptotic pathways via Akt phosphorylation (Berton et al., 2005). To determine whether the impaired integrin clustering we observed in *Was*$^{-/-}$ PMNs correlated with reduced integrin intracellular signaling, we examined Ca^{2+} responses and tyrosine phosphorylation events in wt versus *Was*$^{-/-}$ PMNs. Plating on either fibrinogen- or ICAM-1-coated surfaces produced an obvious and transient Ca^{2+} response in wt but not *Was*$^{-/-}$ PMNs (Figure 7A). In contrast, Ca^{2+} flux responses induced by fMLP stimulation of suspended cells were equivalent in both wt and *Was*$^{-/-}$ cells (data not shown).

Plating PMNs on poly-RGD-coated surfaces led to activation of Erk1 and Erk2 in wt but not *Was*$^{-/-}$ PMNs (Figure 7B). In contrast, Erk1 and Erk2 activation occurred normally in fMLP-stimulated *Was*$^{-/-}$ cells in suspension. Syk, Pyk2, Vav-1, and Cbl phosphorylation were reduced in *Was*$^{-/-}$ PMNs after adhesion to poly-RGD-coated surfaces in the presence of TNF-α. As seen in the Erk pathway, both fMLP- and integrin-mediated adhesion can lead to formation of phospho-Akt; however, only the integrin-mediated pathway was affected in *Was*$^{-/-}$ cells. Together, these data demonstrate that most of the downstream pathways and functional responses induced by chemoattractant signaling (except induction of actin polymerization; Figure S3)

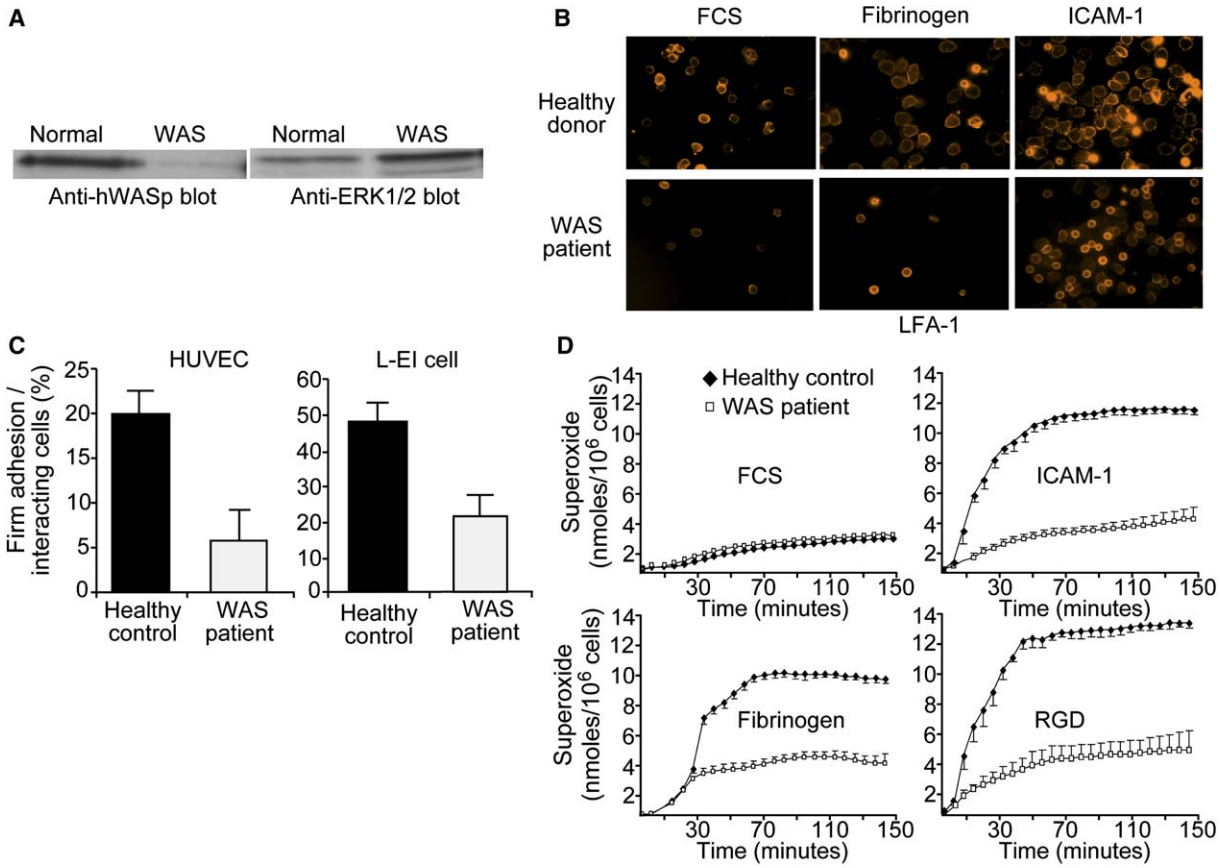

Figure 6. PMNs from a Human WAS Patient Demonstrate Impaired Integrin Clustering, Reduced Adhesion under Shear Flow, and Poor Integrin-Mediated Activation

(A) Peripheral blood PMNs (5×10^6) isolated from a healthy donor or a WAS patient (both >90% purity judged by flow cytometry) were lysed and blotted with anti-human WASp. Filters were stripped and reprobed with anti-Erk1 and Erk2 to confirm equal loading.

(B) Peripheral blood PMNs from a healthy donor or the WAS patient were plated on FBS or human ICAM-1-coated coverslips, fixed, and then stained as described for murine samples in Figure 1.

(C) Peripheral blood PMNs from healthy donors or the WAS patient were injected into a parallel plate flow chamber and passed over monolayers of either TNF-α-treated HUVEC cells or L-EI cells at a shear of 1 dyne/cm^2 for 1 min. Video recordings were then taken at 0.5 s intervals and the numbers of adherent cells was counted as described in Figure 3. Data shown are mean ± SD, n = 3–5 separate microscopy fields and representative of three independent experiments.

(D) Normal donor or WAS patient PMNs were plated on microtiter wells coated with the indicated ligands, in the presence of TNF-α (10 ng/ml) and superoxide production monitored as indicated in Figure 5. Data shown are mean, n = 3 wells each and are representative of three independent experiments. Error bars are ± SD. **p < 0.01, ***p < 0.001 compared to wt.

were normal in *Was*$^{-/-}$ cells; however, pathways downstream from leukocyte integrins after ligand engagement and clustering were severely diminished.

To begin to address the basis for the impaired integrin clustering and signaling defects in *Was*$^{-/-}$ cells, we examined whether the altered cytoskeletal responses of WASp-deficient PMNs resulted in impaired distribution of integrins and key signaling molecules. Colocalization of β2 integrins with phospho-Syk and phospho-Pyk2 in the uropod regions of fully polarized cells was observed in wt PMNs spreading on ICAM-1-coated surfaces but not in *Was*$^{-/-}$ PMNs (Figure S4A). In contrast, WASp did not colocalize with either LFA-1 or Mac-1 in ICAM-1 adherent neutrophils (Figure S4B). Additionally, pharmacologic inhibition of PI3-kinase activity also blocked Mac-1 and LFA-1 clustering, producing a phenotype similar to *Was*$^{-/-}$ cells or to treatment with cytochalasin D (Figure S5). Overall, the correlation of impaired cytoskeletal responses, poor integrin signaling, and mislocalization of key signaling molecules at adhesion sites with the impaired β2 integrin clustering in *Was*$^{-/-}$ cells suggests that a signaling loop between the integrins and the cytoskeleton is impaired in WASp-deficient cells.

The above results suggest that changes in the actin cytoskeleton caused by WASp deficiency affect integrin "outside-in" signaling. To address whether altered cytoskeletal structures affect integrin affinity modulation ("inside-out" signaling), we performed staining of peripheral blood PMNs from our WAS patient with mAb327C, a reporter of the high-affinity conformation of human CD18 (Lupher et al., 2001). Over a dose range of fMLP, we found no effect on integrin affinity modulation in this patient's PMNs as compared to a healthy control donor (Figure S6). These data, together with the observation that mouse PMNs can adhere to high-density ICAM-1-coated beads, suggest that integrin "inside-out" signaling and a shift to high affinity is likely

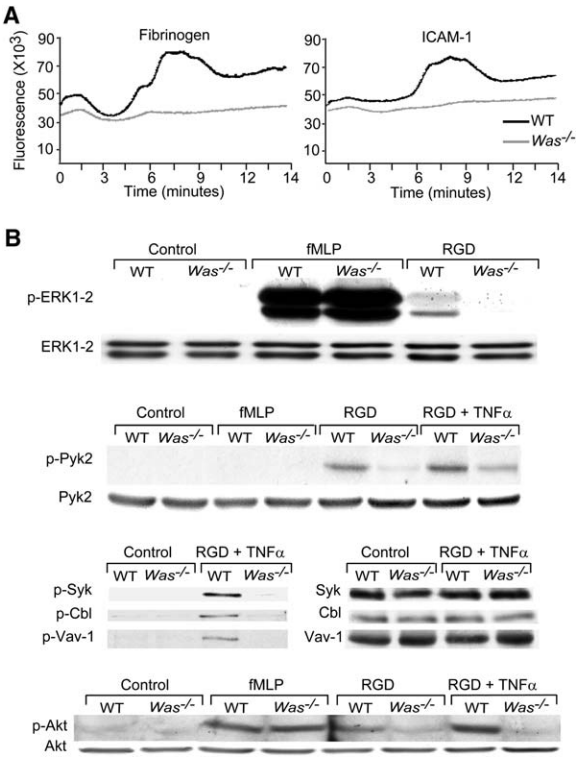

Figure 7. Reduced Integrin-Mediated Signaling in *Was*$^{-/-}$ PMNs

(A) Wild-type and *Was*$^{-/-}$ PMNs loaded with fluo-3 (2×10^6 cells in 100 μl) were plated on fibrinogen- or ICAM-1-coated microtiter plates at 37°C, and fluorescence at 530 nm was monitored every 0.5 s. Data shown are representative of four independent experiments.

(B) Wild-type and *Was*$^{-/-}$ PMNs (1.5×10^7 cells in 2 ml) were plated on RGD-coated tissue culture plates (in the presence or absence of TNF-α at 50 ng/ml) for 30 min. Control samples were unplated and some samples were stimulated with fMLP (3 μM) in suspension. After stimulation, whole-cell lysates were prepared and immunoblotted with phospho-specific anti-Erk1 and Erk2 or anti-Akt, then reprobed with total Erk1-2 or Akt to confirm equivalent loading. Phosphorylation of Pyk 2, Cbl, Syk, and Vav-1 was determined by immunoprecipitation of each protein followed by blotting for phosphotyrosine. Blots were reprobed with anti-Pyk2, Cbl, Syk, or Vav-1 to confirm equal loading. Data shown are representative of three to five separate experiments.

unaffected by reduced actin polymerization resulting from WASp deficiency.

Discussion

In this study, we report that WASp-deficient murine PMNs have defects in actin cytoskeletal function resulting in impaired clustering of β2 integrins after adhesion. As a result, formation of LFA-1 clusters is reduced in *Was*$^{-/-}$ PMNs, which is correlated with reduced cell arrest and transendothelial migration in shear flow. Poor clustering of Mac-1 in the *Was*$^{-/-}$ cells leads to reduced outside-in signaling of effector functions including degranulation and respiratory burst. A similar phenotype was observed in peripheral blood PMNs from a Wiskott-Aldrich Syndrome patient. The capacity for β2-integrins to mediate attachment and chemotaxis was not completely defective and only became manifest under conditions of physiologic shear flow. In the absence of applied shear stress, the integrin redistribution defects associated with WASp deficiency were also manifest, but the impaired adhesive outcome of these defects is simply better reflected in shear flow assays. This may explain why previous investigators have reported normal chemotaxis of PMNs from WAS patients—because the experiments were done under static conditions (Zicha et al., 1998). In vivo, these defects in WASp-deficient PMN adhesion and activation are likely to be quite substantial. Therefore, the relative contribution of PMN dysfunction to the overall immunodeficiency in WAS patients may have been previously underestimated.

The underlying cell biologic defect in *Was*$^{-/-}$ PMNs, macrophages, and DCs may be quite similar, despite that fact that the phenotypes of these cells seem at first glance to be different. The primary defect in WASp-deficient macrophages and DCs is an inability to form podosomes, which are specialized areas of contact between the cell and substratum that serve as points of enrichment for cell adhesion molecules (Burns et al., 2004a). As a result, WASp-deficient DCs fail to cluster their β2 integrins appropriately and display defects in adhesion strengthening (Burns et al., 2004b). This reduced adhesive capacity likely contributes to impaired chemotaxis of *Was*$^{-/-}$ macrophages and DCs, under standard static conditions, as well as the reduced homing capacity of WASp-deficient DCs in vivo (de Noronha et al., 2005). However, PMNs do not form podosomes as a mechanism for cell attachment or adhesion. Like mononuclear cells, PMNs also depend on the ability to form clusters of high-affinity integrins for normal adhesive function, and when this is disrupted (for example, after pharmacologic blockade of the shift to high-affinity sites) (Green et al., 2006), defects in integrin-mediated activation result. Unlike mononuclear cells, it appears that aggregation of integrins may not be required for chemotactic responses of PMNs under static conditions. Thus, normal chemotaxis responses are seen in PMNs from mice lacking the major signaling molecules downstream from the integrins, such as Src-family and Syk kinase-deficient cells or Vav1-Vav3 double mutant cells (Gakidis et al., 2004; Mocsai et al., 2002). In all cases, it has been proposed that only minimal adhesive function (i.e., cell attachment) is required for the PMN to be able to mount a migratory response in standard Boyden chamber type chemotaxis assay. The fact that macrophages and DCs require more complex adhesive structures (i.e., podosomes) to mount migratory responses in culture, whereas PMNs apparently do not, may be the simple explanation for the different chemotactic responses between *Was*$^{-/-}$ macrophages/dendritic cells and PMNs.

The impairment in endothelial transmigration present in *Was*$^{-/-}$ cells is not surprising given the clear role for β2 integrins in this process. A number of studies have demonstrated that coordinate redistribution of endothelial ICAM-1 and PMN β2 integrins into ring-like or cup-like structures is required for efficient trans and paracellular migration (Carman and Springer, 2004; Shaw et al., 2004). Similarly, the presence of chemokines along the apical surface of the endothelial cell as well as the density of β2 ligands (mainly ICAM-1) also influences the rate and mode of transendothelial migration (Cinamon et al., 2004). Given the obvious defect in β2 integrin clustering in *Was*$^{-/-}$ PMNs, it will be important to examine

their ability to mobilize to other inflammatory sites in both autoimmune and infectious disease models.

In this report, we have concentrated on those signaling response and functions that are downstream of integrin ligation. However, it is likely that the WASp is also involved in integrating signals from other PMN receptors as well. In this regard, we can comment on the role of WASp in GPCR signaling. As expected, stimulation of *Was*$^{-/-}$ PMNs with chemokines or chemoattractants (MIP-1α, MIP-2, or fMLP) failed to induce substantial actin-polymerization responses. However, a number of GPCR agonists induced normal chemotaxis, degranulation, respiratory burst, and intracellular signaling responses in suspended *Was*$^{-/-}$ cells. Similarly, fMLP stimulated increased binding to high-density coated ICAM-1 beads and produced normal integrin affinity modulation via reporter mAb staining in WASp-deficient human PMNs. Hence, it appears that many of the primary signaling responses from GPCRs do not depend on WASp function.

Our observations support the conclusion that WASp is mainly involved in "oustide-in" integrin signaling pathways. At first glance, the impaired proximal integrin signaling events (tyrosine kinase activation) in *Was*$^{-/-}$ cells may appear to be unexpected, since actin polymerization responses requiring WASp should be downstream from tyrosine phosphorylation. However, it may be somewhat simplistic to view "outside-in" integrin signaling as a sequential and linear pathway that is occurring simultaneously from all receptors in the cell. It is more likely that initial integrin engagement induces membrane-localized kinase activation and actin polymerization, which in turn activates signaling leading to more integrin clustering and further integrin signaling—in the fashion of a circular feed-forward loop pathway. Lack of WASp blocks this signal amplification. Therefore, while our observations appear to demonstrate a very early proximal defect in the integrin-signaling pathway (leading to poor activation and localization of tyrosine kinases) as the underlying cause of the PMN dysfunction in WASp-deficient cells, it is perhaps more accurate to think of the pathway as failing to amplify a signaling loop.

Overall, these results demonstrate that like other cells in the innate immune system, PMNs are highly dependent on WASp for normal function. It will be an important question for future work to determine how much of the overall immune deficiency caused by lack of this protein is due to PMN dysfunction. In mouse models, lineage-specific ablation of WASp will be the next step to answering this question.

Experimental Procedures

Mice

CD18- and CD11b-deficient mice were purchased from Jackson Laboratory. *Was*$^{-/-}$ mice, originally made by Snapper et al. (1998), were kindly provided by Dr. Arie Abo (PPD Pharmaceuticals, Foster City, CA). Animals were kept in a specific pathogen-free facility at UCSF and used according to protocols approved by the UCSF Committee on Animal Research. The original *Was*$^{-/-}$ mice were backcrossed to C57BL/6 background for four generations, and all experiments were performed with the backcrossed animals.

Reagents and mAbs

Recombinant murine or human TNF-α (from Becton Dickinson), fMLP, PAF, LTB4, and C5a (from Sigma) were used at 10–20 ng/ml, 3 μM, 1 μM, 15 nM, and 50 ng/ml, respectively. Cytochalasin D (from Sigma) was used at the indicated doses. Poly-RGD peptides (Calbiochem), human plasma fibrinogen (ICN Biomedicals), and collagen (Sigma) were used to coat plates as previously described (Pereira and Lowell, 2003). PNAd (MECA-79-reactive ligands, known as the peripheral node addressins from human tonsil) was kindly provided by S. Rosen (UCSF). Anti-Mac-1 (CD11b, clone M1/70), anti-LFA-1 (CD11a, clone M17/4), and non-blocking anti-LFA-1 (clone 2D7) were from Becton Dickinson/Pharmingen. Phospho-ERK1/2, phospho-Akt, phospho-JNK, phospho-p38, phospho-Pyk2, and phospho-Syk were purchased from Cell Signaling. Anti-WAS monoclonal antibody gelatin-free antibody (for labeling with Alexa647 according to Molecular Probes protocol), anti-ERK1/2, Cbl, Vav-1, human WASp, and Pyk2 polyclonal Abs were purchased from Santa Cruz Biotechnology.

PMN Isolation and Cell Lines

Murine bone marrow PMNs were isolated with a one-step 62% density gradient medium, as previously described (Pereira and Lowell, 2003). Human peripheral blood PMNs were isolated by dextran sedimentation of RBCs, followed by pelleting in Ficoll-Paque Plus (Amersham). The murine bEND.3 cell line, a brain capillary endothelial cell line immortalized by retroviral transduction with polyoma middle T antigen, was kindly provided by Dr. Eric Brown (UCSF). Transfected L-cells coexpressing E-selectin and ICAM-1 (L-EI) and human umbilical vein endothelial cells (HUVECs) were maintained as described (Green et al., 2004).

Fixed and Live Cell Immunofluorescence Microscopy

PMN integrin clustering was determined by plating cells (2.5×10^5/ml in 150 μl) on coverslips coated with the indicated proteins at 37°C for 10 min, followed by fixing in 2% paraformaldehyde for 10 min (at 37°C), then staining for CD11a or CD11b. PMN clustering induced by binding to bEND.3 cells was determined by plating cells for 20 min on coverslips on which a monolayer of bEND.3 cells had been activated by incubation with TNF-α for 4 hr prior to use. Integrin clusters were counted with Image J (NIH) analysis software. Regions of discontinuous membrane integrin staining of at least 3-fold above background were defined as integrin clusters.

The topography of LFA-1 and Mac-1 was imaged in real time with alternating DIC/fluorescence video microscopy during PMN arrest in shear flow. PMNs were stained with Alexa488-conjugated anti-Mac-1 (clone M1/70) or nonblocking anti-LFA-1 (clone 2D7) at 20 μg/ml at 4°C for 30 min, then perfused over ICAM-1-coated coverslips at a concentration of 2.5×10^6/ml with a shear force of 0.3 dyne/cm^2 while imaging was initiated. Image acquisition was achieved with an inverted Axiovert 200 M microscope and a ×40/1.4 lens (Carl Zeiss, NJ), equipped with a 175 W xenon high-speed DG4 wavelength selector and a single emission filter wheel (Sutter Instruments, Novato, CA), a PI piezoelectric z-drive (Physik Instrument, Germany), and a cooled-CCD Coolsnap camera (Roper Instruments, NJ). Data were acquired and analyzed with Metamorph (Universal Imaging, Downingtown, PA), and static cell images were analyzed with Image J (NIH) analysis software. For live-cell imaging, data were acquired every 2 s and consisted of single DIC image followed by a 490/20 excitation and 528/38 emission to detect Alexa488 staining. Images were collected over a 200 s period.

PMN Adhesion and Transendothelial Migration under Shear Flow

PMN adhesion under flow conditions was measured in a parallel plate flow chamber, as described previously (Green et al., 2004). Isolated PMNs (10^6/ml) were passed over confluent L-EI monolayers at 1.0 dynes/cm^2 for 1 min at 37°C, after which digital image sequences were acquired with a TE200 microscope (Nikon) equipped with a 40× phase contrast objective and analog CCD camera. Image sequences were captured and analyzed with Image Pro Plus v4.5 (Media Cybernetics). Rolling PMNs were defined as cells having moved greater that one cell diameter in 30 s with velocity computed as the distance rolled divided by the period of time a cell traversed the field of view. Arrested PMNs were defined as those cells that moved less than one cell diameter in 30 s. The fractions of rolling and arrested cells were determined by normalizing to the total number of PMNs interacting with the L-EI or bEND.3 cell monolayer, both

adherent and rolling, present in the field of view. Transendothelial migration was determined by passing PMNs over L-EI or bEND.3 cell monolayers, stimulated with murine TNF-α (10 ng/ml) for 4 hr prior. Transendothelial migration was assessed by counting the number of fully arrested PMNs that migrated to the junction between endothelial cells and then transitioned to phase darkness as they migrated below the endothelial monolayer.

ICAM-1 Bead Binding Assay

Quantitative binding of ICAM-1-coated latex beads to murine PMNs was performed as described (Lum et al., 2002; Tsang et al., 1997). Fluorescent latex beads (1 μm diameter, Molecular Probes) were coated with recombinant ICAM-1-Fc at 20 and 70 μg/ml. PMNs were mixed with ICAM-1-coated beads in sample volumes of 200 μl (HEPES buffer, 1.5 mM $CaCl_2$) containing 10^6 PMNs with 2×10^7 beads in FACs test tubes with a small magnetic stirring bar. Samples were run on the flow cytometer for 1 min to establish a baseline reading, and then fMLP was added to 5 μM and cells were analyzed continuously for 5 min while being stirred at a shear stress of 1.0 dyne/cm^2. Binding of ICAM-1-coated beads was determined by gating on PMNs with FSC/SSC, and the rate of bead capture was determined as described (Lum et al., 2002; Tsang et al., 1997).

PMN Migration In Vivo

PMN migration in vivo was observed in the thioglycollate-induced sterile peritonitis model as described (Gakidis et al., 2004; Mocsai et al., 2002). Since a fraction of *Was*$^{-/-}$ mice have chronic colitis and hematocelia starting around 4 months of age (Snapper et al., 1998; Zhang et al., 1999), we used 6-week-old mice for this experiment. Any mice with evidence of hematocelia after thioglycollate were not included in the data analysis.

PMN Functional Assays

Adhesion-dependent respiratory burst and degranulation assays were performed essentially as described (Lowell et al., 1996; Mocsai et al., 1999; Pereira and Lowell, 2003). Coating of 96-well tissue culture plates was done with fibrinogen (10 μg/ml), poly-RGD peptide (20 μg/ml), ICAM-1 (0.5 μg/ml), or collagen (10 μg/ml). Monolayers of bEND.3 cells were obtained by culturing cells in 96-well plates until completely confluent. Adherent respiratory burst was measured by a cytochrome C reduction, while degranulation of the secondary granule marker lactoferrin was determined by ELISA from cell supernatants.

Assays of Integrin Signaling

Adhesion-dependent calcium flux was determined by fluo-3 loading cells as described (Zhang et al., 2005) followed by plating in microtiter wells precoated with fibrinogen or ICAM-1. Calcium flux was measured by Mithras LB 940 plate reader with 480 excitation and 530 emission every 0.5 s for 15 min. Adhesion-dependent phosphorylation of Erk1, Erk2, Pyk2, Syk, Cbl, Vav-1, or Akt was determined as previously described (Zhang et al., 2005). PMNs (10^7 cells in 2 ml of HBSS with Ca^{2+}/Mg^{2+}) were allowed to adhere to poly-RGD-coated 35 mm dishes for 30 min in either the presence or absence of TNF-α at 37°C in a 5% CO_2 incubator. Attached cells were lysed by addition of RIPA buffer before immunoprecipitation with antibody to Pyk2, Syk, Vav-1, or Cbl, separation by SDS-PAGE, and detection of tyrosine phosphorylated proteins by Western blotting with mAb 4G10 antibody. Immunoprecipitations were controlled for equal loading by stripping the blotting membrane and reprobing with the same Ab as used for precipitation. For detection of ERK1/2, p38, and JNK phosphorylation, PMN lysates were separated by SDS-PAGE, followed by Western blotting with phospho-specific ERK1/2, phospho-p38, and phospho-JNK antibodies.

Supplemental Data

Supplemental Data include six figures and eight movies and can be found with this article online at http://www.immunity.com/cgi/content/full/25/2/285/DC1/.

Acknowledgments

We thank Clare Abram, Jessica Van Ziffle, and members of the Eric Brown and Tony DeFranco laboratories who provided thoughtful discussions and critiques through out this project. We thank Dr. Neetu Gupta, Wouter Hazenbos, Tomas Brdicka, Matthew F. Krummel, Jordan Jacobelli, Rachel Friedman, Lenny Dragone, Michelle Herminston, Kenji Uchimura, Mark S. Singer, Sheena Kerr, and Guy Cinamon for helpful discussion and technical assistance. Supported by NIH grants AI65495 and AI68150 to C.A.L. and AI47294 to S.I.S. C.E.G. is supported by NIH/NHLBI NRSA postdoctoral training fellowship T32-HL07013-26. C.A.L. is a Scholar of the Leukemia and Lymphoma Society. S.I.S. is an established investigator of the American Heart Association.

Received: February 8, 2006
Revised: May 4, 2006
Accepted: June 6, 2006
Published online: August 10, 2006

References

Badolato, R., Sozzani, S., Malacarne, F., Bresciani, S., Fiorini, M., Borsatti, A., Albertini, A., Mantovani, A., Ugazio, A.G., and Notarangelo, L.D. (1998). Monocytes from Wiskott-Aldrich patients display reduced chemotaxis and lack of cell polarization in response to monocyte chemoattractant protein-1 and formyl-methionyl-leucyl-phenylalanine. J. Immunol. *161*, 1026–1033.

Badour, K., Zhang, J., and Siminovitch, K.A. (2004). Involvement of the Wiskott-Aldrich syndrome protein and other actin regulatory adaptors in T cell activation. Semin. Immunol. *16*, 395–407.

Berton, G., Mocsai, A., and Lowell, C.A. (2005). Src and Syk kinases: key regulators of phagocytic cell activation. Trends Immunol. *26*, 208–214.

Bunting, M., Harris, E.S., McIntyre, T.M., Prescott, S.M., and Zimmerman, G.A. (2002). Leukocyte adhesion deficiency syndromes: adhesion and tethering defects involving β2 integrins and selectin ligands. Curr. Opin. Hematol. *9*, 30–35.

Burns, S., Cory, G.O., Vainchenker, W., and Thrasher, A.J. (2004a). Mechanisms of WASp-mediated hematologic and immunologic disease. Blood *104*, 3454–3462.

Burns, S., Hardy, S.J., Buddle, J., Yong, K.L., Jones, G.E., and Thrasher, A.J. (2004b). Maturation of DC is associated with changes in motile characteristics and adherence. Cell Motil. Cytoskeleton *57*, 118–132.

Carman, C.V., and Springer, T.A. (2004). A transmigratory cup in leukocyte diapedesis both through individual vascular endothelial cells and between them. J. Cell Biol. *167*, 377–388.

Cinamon, G., Shinder, V., Shamri, R., and Alon, R. (2004). Chemoattractant signals and β2 integrin occupancy at apical endothelial contacts combine with shear stress signals to promote transendothelial neutrophil migration. J. Immunol. *173*, 7282–7291.

de Noronha, S., Hardy, S., Sinclair, J., Blundell, M.P., Strid, J., Schulz, O., Zwirner, J., Jones, G.E., Katz, D.R., Kinnon, C., and Thrasher, A.J. (2005). Impaired dendritic-cell homing in vivo in the absence of Wiskott-Aldrich syndrome protein. Blood *105*, 1590–1597.

Ding, Z.M., Babensee, J.E., Simon, S.I., Lu, H., Perrard, J.L., Bullard, D.C., Dai, X.Y., Bromley, S.K., Dustin, M.L., Entman, M.L., et al. (1999). Relative contribution of LFA-1 and Mac-1 to neutrophil adhesion and migration. J. Immunol. *163*, 5029–5038.

Gakidis, M.A., Cullere, X., Olson, T., Wilsbacher, J.L., Zhang, B., Moores, S.L., Ley, K., Swat, W., Mayadas, T., and Brugge, J.S. (2004). Vav GEFs are required for β2 integrin-dependent functions of neutrophils. J. Cell Biol. *166*, 273–282.

Green, C.E., Pearson, D.N., Camphausen, R.T., Staunton, D.E., and Simon, S.I. (2004). Shear-dependent capping of L-selectin and P-selectin glycoprotein ligand 1 by E-selectin signals activation of high-avidity β2-integrin on neutrophils. J. Immunol. *172*, 7780–7790.

Green, C.E., Schaff, U.Y., Sarantos, M.R., Lum, A.F., Staunton, D.E., and Simon, S.I. (2006). Dynamic shifts in LFA-1 affinity regulate neutrophil rolling, arrest, and transmigration on inflamed endothelium. Blood *107*, 2101–2111.

Jones, G.E., Zicha, D., Dunn, G.A., Blundell, M., and Thrasher, A. (2002). Restoration of podosomes and chemotaxis in Wiskott-Aldrich syndrome macrophages following induced expression of WASp. Int. J. Biochem. Cell Biol. *34*, 806–815.

Kolluri, R., Shehabeldin, A., Peacocke, M., Lamhonwah, A.M., Teichert-Kuliszewska, K., Weissman, S.M., and Siminovitch, K.A. (1995). Identification of WASP mutations in patients with Wiskott-Aldrich syndrome and isolated thrombocytopenia reveals allelic heterogeneity at the WAS locus. Hum. Mol. Genet. *4*, 1119–1126.

Lowell, C.A., Fumagalli, L., and Berton, G. (1996). Deficiency of Src family kinases p59/61^{hck} and p58$^{c\text{-}fgr}$ results in defective adhesion-dependent neutrophil functions. J. Cell Biol. *133*, 895–910.

Lum, A.F., Green, C.E., Lee, G.R., Staunton, D.E., and Simon, S.I. (2002). Dynamic regulation of LFA-1 activation and neutrophil arrest on intercellular adhesion molecule 1 (ICAM-1) in shear flow. J. Biol. Chem. *277*, 20660–20670.

Lupher, M.L., Jr., Harris, E.A., Beals, C.R., Sui, L.M., Liddington, R.C., and Staunton, D.E. (2001). Cellular activation of leukocyte function-associated antigen-1 and its affinity are regulated at the I domain allosteric site. J. Immunol. *167*, 1431–1439.

Mocsai, A., Ligeti, E., Lowell, C.A., and Berton, G. (1999). Adhesion-dependent degranulation of neutrophils requires the Src family kinases Fgr and Hck. J. Immunol. *162*, 1120–1126.

Mocsai, A., Zhou, M., Meng, F., Tybulewicz, V.L., and Lowell, C.A. (2002). Syk is required for integrin signaling in neutrophils. Immunity *16*, 547–558.

Pereira, S., and Lowell, C. (2003). The Lyn tyrosine kinase negatively regulates neutrophil integrin signaling. J. Immunol. *171*, 1319–1327.

Shaw, S.K., Ma, S., Kim, M.B., Rao, R.M., Hartman, C.U., Froio, R.M., Yang, L., Jones, T., Liu, Y., Nusrat, A., et al. (2004). Coordinated redistribution of leukocyte LFA-1 and endothelial cell ICAM-1 accompany neutrophil transmigration. J. Exp. Med. *200*, 1571–1580.

Simon, S.I., and Green, C.E. (2005). Molecular mechanics and dynamics of leukocyte recruitment during inflammation. Annu. Rev. Biomed. Eng. *7*, 151–185.

Snapper, S.B., Rosen, F.S., Mizoguchi, E., Cohen, P., Khan, W., Liu, C.H., Hagemann, T.L., Kwan, S.P., Ferrini, R., Davidson, L., et al. (1998). Wiskott-Aldrich syndrome protein-deficient mice reveal a role for WASP in T but not B cell activation. Immunity *9*, 81–91.

Tsang, Y.T., Neelamegham, S., Hu, Y., Berg, E.L., Burns, A.R., Smith, C.W., and Simon, S.I. (1997). Synergy between L-selectin signaling and chemotactic activation during neutrophil adhesion and transmigration. J. Immunol. *159*, 4566–4577.

Zhang, J., Shehabeldin, A., da Cruz, L.A., Butler, J., Somani, A.K., McGavin, M., Kozieradzki, I., dos Santos, A.O., Nagy, A., Grinstein, S., et al. (1999). Antigen receptor-induced activation and cytoskeletal rearrangement are impaired in Wiskott-Aldrich syndrome protein-deficient lymphocytes. J. Exp. Med. *190*, 1329–1342.

Zhang, H., Meng, F., Chu, C.L., Takai, T., and Lowell, C.A. (2005). The Src Family kinases Hck and Fgr negatively regulate neutrophil and dendritic cell chemokine signaling via PIR-B. Immunity *22*, 235–246.

Zicha, D., Allen, W.E., Brickell, P.M., Kinnon, C., Dunn, G.A., Jones, G.E., and Thrasher, A.J. (1998). Chemotaxis of macrophages is abolished in the Wiskott-Aldrich syndrome. Br. J. Haematol. *101*, 659–665.